Fourier Transform Raman Spectroscopy of the Bacteriorhodopsin Mutant Tyr-185→Phe: Formation of a Stable O-like Species during Light Adaptation and Detection of Its Transient N-like Photoproduct†

Parshuram Rath,‡ Mark P. Krebs,§ Yiwu He,‡ H. Gobind Khorana,§ and Kenneth J. Rothschild*,‡

Physics Department and Program in Cellular Biophysics, Boston University, Boston, Massachusetts 02215, and Departments of Biology and Chemistry, Massachusetts Institute of Technology, Cambridge, Massachusetts 02139

Received July 20, 1992; Revised Manuscript Received December 18, 1992

ABSTRACT: Near-infrared FT-Raman spectroscopy can be used to measure the vibrations of the bacteriorhodopsin (bR) chromophore without the disadvantage of conventional visible resonance Raman spectroscopy, where the visible excitation drives the bR photoreactions. We utilized this technique to investigate the light–dark adaptation of bacteriorhodopsin and the mutant Tyr-185→Phe (Y185F) at room temperature in solution. Compared to wild-type bR, both the FT-Raman and resonance Raman spectra of the light-adapted Y185F displayed new features characteristic of the vibrations of the O intermediate. Light adaptation of Y185F was found to involve a 13-cis, C=N syn→all-trans isomerization of the retinal chromophore which produces a species similar to bR_{570} and a second O-like species. Dark adaptation, which was much slower in Y185F compared to wild-type bR, involved a parallel decay of the bR_{570} and O-like species and resulted in a decreased all-trans:13-cis ratio compared to wild type. Further evidence for the existence of an O-like species in Y185F comes from pump–probe Raman difference spectroscopy, where a red pump beam is found to produce a species very similar to the N intermediate in the photocycle. This species is shown by stroboscopic Raman measurements to exist transiently even at high pH. We postulate that when the Y185F chromophore has an all-trans structure the effective pK_a of Asp-85 and Asp-212 is elevated in Y185F due to the disruption of the Asp-212/Tyr-185 hydrogen bond, thereby accounting for the increased protonation of these residues in the O-like species.

Bacteriorhodopsin (bR)[1] is an integral membrane protein found in the purple membrane of the extremely halophilic *Halobacterium halobium* (Oesterhelt & Stoeckenius, 1971; Stoeckenius & Bogomolni, 1982). Upon absorption of a photon, bR undergoes a photocycle involving a series of intermediates: K_{630}, L_{550}, M_{412}, N_{550}, and O_{640}, each with its characteristic absorption maximum. In this process, a net proton is transported across purple membrane from the inside to the outside of the cell. Although the kinetics and visible absorption of each of these intermediates have been well characterized, their exact role in the proton transport mechanism is not yet completely understood.

One approach to elucidating the mechanism of proton pumping in bR is the application of vibrational spectroscopy. Resonance Raman spectroscopy (RRS) provides a means to study the structure of various retinylidene chromophores including those of bR and its photointermediates by selectively enhancing their vibrations [for reviews, see, e.g., Callender and Honig (1977), Warshel (1977), and Mathies et al. (1991) and references cited therein]. This work has resulted in a comprehensive picture of the structural changes which occur in the chromophore during the bR photocycle (Smith et al., 1985; Mathies et al., 1991). However, the photoreactivity of bR is an inherent problem in these studies since the visible wavelength of the exciting light is absorbed by the chromophore and drives the photoreactions of bR and its intermediates. While this problem can be alleviated by using low-power excitation and spinning or flowing the sample past the exciting laser beam (Callender et al., 1976; Mathies et al., 1976; Stockburger et al., 1979; Argade & Rothschild, 1982), this approach requires large sample volumes and can result in artifacts due to the possibility of long-lived and sometimes irreversible photoreactions. For these reasons, it is desirable to probe the vibrations of the chromophore without the use of visible light.

In contrast to RRS, Fourier transform infrared (FTIR) difference spectroscopy offers a means to measure the vibrations of both chromophore and protein without visible light (Rothschild et al., 1981; Bagley et al., 1982; Siebert & Mäntele, 1983; Rothschild, 1992). This approach has been especially valuable when combined with isotope labeling and site-directed mutagenesis (Engelhard et al., 1985; Braiman et al., 1988a,b; Gerwert et al., 1989; Maeda et al., 1992) and has resulted in information about protonation changes of individual amino acid residues.

In this work, we have used a third method, Fourier transform Raman (FT-Raman) spectroscopy, for measuring the vibrational spectrum of the bR chromophore. Since the wavelength of the exciting light is in the near-infrared region, photoreactions of light-adapted and dark-adapted bR are avoided. As previously reported (Johnson & Rubinovitz, 1990; Sawatzki et al., 1990), sufficient resonance enhancement (preresonance) of bR occurs so that all of the chromophore vibrations detected by conventional resonance Raman spectroscopy are also detected in the FT-Raman spectrum. In contrast, Raman

† This work was supported by grants from the NSF (DMB-9106017), NIH (EY05499), and ONR (N00014-88-K-0464) to K.J.R. and from the NIH (GM28289 and AI11479) to H.G.K.

* Address correspondence to this author.

‡ Boston University.

§ Massachusetts Institute of Technology.

[1] Abbreviations: bR, bacteriorhodopsin; FT-Raman, Fourier transform Raman; RRS, resonance Raman spectroscopy; FTIR, Fourier transform infrared; FWHM, full width at half-maximum; WT, wild type; HOOP, hydrogen out-of-plane; BM^T, all-trans component of the acid-induced blue membrane; BM^C, 13-cis component of the acid-induced blue membrane.

0006-2960/93/0432-2272$04.00/0

scattering from protein vibrations is absent or weak (especially for bR), and thereby does not interfere with assignment of chromophore vibrational modes.

In our first application of this approach, we have studied the light–dark adaptation of the wild-type bR and the mutant Y185F.[2] In a related paper, we have shown that there exists a red-shifted species in light-adapted Y185F that has a vibrational spectrum similar to the O intermediate in the photocycle of wild-type bR (He et al., 1993). However, since the O-like species (O^{Y185F}) was measured by low-temperature FTIR difference spectroscopy in hydrated films, characterization of this red-shifted species at room temperature and in solution is still necessary (Sonar et al., 1993). Our present results show that an O-like species is formed upon light adaptation of Y185F in solution at room temperature. Parallel FT-Raman and FTIR difference spectra of this process reveal that both the O^{Y185F} and bR_{570}-like species (bR_{570}^{Y185F})[3] are formed from a 13-cis, C=N syn containing bR_{555}-like species (bR_{555}^{Y185F}). However, unlike bR_{570}, the O^{Y185F} species has protonated Asp-85 and Asp-212 residues. The O^{Y185F} and bR_{570}^{Y185F} species decay in dark in parallel. However, the rate of dark adaptation of Y185F is significantly slower than wild-type bR and results in an increased amount of the 13-cis, C=N syn species. Photoexcitation of the O^{Y185F} species with red light produces a transient N-like intermediate. These results are discussed in terms of the chromophore configuration and protonation states of some of the key active-site residues of bR.

MATERIALS AND METHODS

The mutant protein was expressed from an *H. halobium* strain bearing a chromosomal *bop* gene containing the Y185F mutation as previously described (Bousché et al., 1992). Detailed discussion of this procedure is given in the preceeding paper (Sonar et al., 1993).

FT-Raman Spectroscopy. FT-Raman measurements were made using an FTS 40 spectrometer (Bio-Rad, Digilab Division, Cambridge, MA) equipped with a quartz beam splitter and FT-Raman accessory. Signal detection was performed using a liquid nitrogen cooled germanium detector, with a standard filter for cosmic ray signals. The 1064-nm beam from a CW Nd:YAG laser (Model SL501P, Spectron Laser) operating at 750-mW power level was used for Raman excitation.

Typically, a 200-μL sample (in distilled water containing 3 mM NaN_3) at a concentration giving a visible absorbance at 570 nm of 12 ODU was placed in a 0.4-mm i.d. glass tube, and Raman signals were collected using 180° back-scattering optics. Dark-adapted wild-type bR samples were kept at room temperature or in the refrigerator for several hours prior to placing them in the spectrometer. In the case of Y185F, which has a much slower dark adaptation, samples were kept at room temperature in the dark for more than 20 h and in the refrigerator in the dark for over 1 week. Light adaptation was accomplished using a 150-W fiber optic illuminator (Dolan-Jenner Industries Inc., Woburn, MA) and a combination of a 505-nm long-pass filter and a 600-nm short-pass filter (Corion Corp., Holiston, MA). The measurements of light-adapted samples consisted of a cycle of 2-minute scans in the dark followed by 5 min of light adaptation. Dark-adapted samples were recorded in the absence of visible light. All spectra were recorded at either 4- or 8-cm^{-1} resolution as indicated.

Resonance Raman Spectroscopy. A 300-μL volume sample was placed in a cylindrical quartz cell of 19-mm internal diameter and spun at the rate of 45 Hz. The sample was excited either by the 568.2-nm laser beam from a Krypton ion laser (Coherent Model I200 K-2) or by the 514.5-nm laser beam from an Argon ion laser (Model I70-4, Coherent Inc., Palo Alto, CA). The laser beam was cylindrically focused and directed parallel to the rotation axis of the spinning cell, and the scattered radiation was collected at a right angle from the incident beam as described previously (Argade & Rothschild, 1982). Laser power was kept at a minimum to obtain low photoalteration of the sample (Mathies et al., 1976; Callender et al., 1976; Mathies, 1979; Deng et al., 1985), typically less than 5%. The period of rotation was 22 ms, and the sample transit time through the probe beam was less than 1.8 μs.

The Raman spectrometer consisted of a 0.5-m single-grating monochromator (Model 500M, SPEX Industries, Edison, NJ) and a Model 1420 EG&G PAR enhanced optical multichannel analyzer (OMA) connected to a Model 1461 detector controller (EG&G PAR, Princeton, NJ). The detector was cooled to −20 °C. Data analysis was performed using the software LabCalc (Galactic Industries, Nashua, NH). A simple two-point averaging was performed on all data to correct for the differences in gain between odd and even pixels of the photodiode array detector. The spectra were calibrated using the known peak frequencies of a toluene spectrum. The spectral resolution were 5 and 4 cm^{-1} at 514.5- and 568.2-nm excitations, respectively.

(A) Pump–Probe Measurements. For these measurements, the 514.5-nm laser beam from the Argon laser (typically 5 mW at the sample) was used as the probe beam, and the 647.1-nm red laser beam (100 mW at sample) from the Krypton laser was used as the pump beam. The pump beam was cylindrically focused upstream from the probe beam onto the spinning cell at a temporal separation of 5 ms. In this case, only photoproducts generated by the red pump beam (e.g., the N intermediate; see Results) which have a lifetime longer than the temporal separation between the pump and the probe beam (5 ms) will be detected in significant concentration. Spectra were recorded without (probe-only) and with (pump+probe) the pump beam. The probe-only spectrum was subtracted from the pump+probe spectrum to obtain the spectrum of the photoproduct created by the pump beam. The subtraction factor was chosen so as to minimize the contribution from the bands in the probe-only spectrum in the difference spectrum without producing any negative bands. The spectrum of the N intermediate of wild-type bR was obtained by subtracting the probe-only spectrum (2 mW, 520.8 nm) of a pH 7 sample in 10 mM Tris buffer from that of the pump (100 mW, 514.5 nm, 8 ms upstream from the probe beam) and probe (2 mW, 520.8 nm) spectrum of a sample in the same buffer at pH 9 in 3 M KCl. Subtraction was performed so that the intensity at 1347 cm^{-1} was minimized (Nakagawa et al., 1991) in the resultant spectrum without producing any negative bands.

(B) Stroboscopic Raman Measurements. A Uniblitz Model LS6Z (A. W. Vincent Associates, Rochester, NY) electronic shutter with Model 100-2B controller was used for stroboscopic measurements. The on–off time of the Raman excitation

[2] Designations for bR mutants make use of the standard one-letter abbreviations for amino acids. Thus, "Y185F" signifies the mutant in which tyrosine at position 185 in the amino acid sequence has been replaced by phenylalanine.

[3] bR_{570}^{Y185F}, bR_{555}^{Y185F}, and O^{Y185F} are the bR_{570}, bR_{555}, and O-like species, respectively, observed in the Y185F mutant of bacteriorhodopsin.

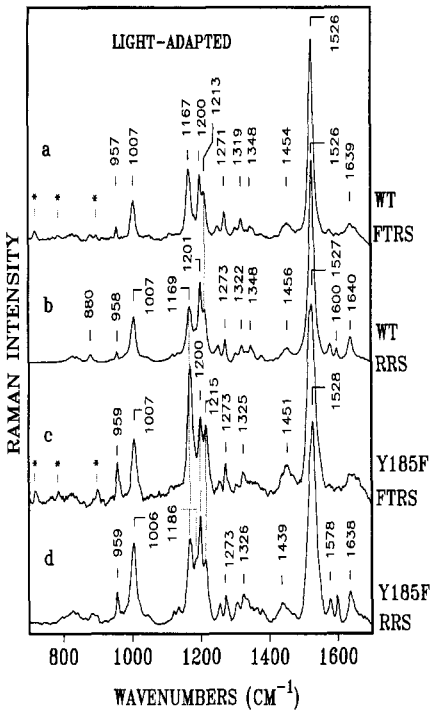

FIGURE 1: FT-Raman and resonance Raman spectra of wild-type bR and the mutant Y185F. Wild-type bR spectra are shown in (a) (FT-Raman) and (b) (resonance Raman), and Y185F spectra are shown in (c) (FT-Raman) and (d) (resonance Raman). All spectra were recorded at room temperature and 4-cm^{-1} spectral resolution. FT-Raman spectra (a and c) were recorded with 750 mW of 1064-nm excitation, whereas resonance Raman spectra (b and d) were obtained from a spinning sample with 5 mW of 568.2-nm laser excitation. The 568.2-nm excitation was preferred over the 514.5 nm (used for later experiments) to favor resonance enhancement of the O species. Bands marked with an asterisk are due to spectrometer artifacts.

(probe beam) and the synchronization of the detector data collection with the probe on time were achieved via the detector controller described above. Typically, the probe beam was switched on for 0.1 s, and data were collected during that period. Then the probe beam was switched off for 1.9 s to allow sufficient time for the photoproduct created by the probe beam to decay. In order to avoid dark adaptation of the samples at pH 9.2 during the course of the stroboscopic measurements, spectra were recorded for 30 min, and then the sample was light-adapted by a 100-mW 568.2-nm laser beam for 5 min. The whole procedure was repeated several times, and the individual spectra were averaged in order to obtain a spectrum with a good signal-to-noise ratio.

FTIR Difference Spectroscopy. Wild-type bR dark→light FTIR difference spectra were measured at 310 K temperature as reported previously (Roepe et al., 1988). For the mutant Y185F, similar difference spectra were recorded at 293 K and 2-cm^{-1} resolution from a sample dark-adapted for more than 24 h and then illuminated with light from a fiber optic illuminator and a 505-nm long-pass filter. A Nicolet Model 740 FTIR spectrometer (Nicolet Analytical Instruments, Madison, WI) was used for this measurement.

RESULTS

Raman Spectra of Light-Adapted bR and the Mutant Y185F. The FT-Raman and resonance Raman spectra of light-adapted wild-type (WT) bR and the mutant Y185F are presented in Figure 1. In the case of the FT-Raman spectroscopy, complete light adaptation was not obtained due to the high concentration of the samples (see Materials and Methods) as indicated by the appearance of a small band at 800 cm^{-1} characteristic of the bR_{555} component of dark-adapted bR (Stockburger et al., 1979; Terner et al., 1979; Smith et al., 1983, 1987a; data not shown). In order to correct for this effect, the spectrum of a fully dark-adapted sample was subtracted until the 800-cm^{-1} band disappeared (Figure 1a,c). The resulting FT-Raman spectrum of bR (Figure 1a) is similar to that of the corresponding resonance Raman spectrum, indicating that the FT-Raman spectrum reflects mainly vibrations of the retinal chromophore in agreement with earlier work (Johnson & Rubinovitz, 1990; Sawatzki et al., 1990). However, several differences should be noted between the FT-Raman and resonance Raman spectra. A broad band near 1639 cm^{-1} due to the O–H bending mode of water partially obscures the 1640-cm^{-1} C=N stretch mode of the chromophore in the FT-Raman spectrum. In addition, there are some differences in the intensity of bands in the two spectra which are expected to be due to the dependence of the cross section for resonance Raman Scattering of a particular mode on the excitation wavelength (Myers et al., 1983) (RRS, 568.2 nm; FT-Raman, 1064 nm). For example, the relative intensities of the C–C stretching modes in the FT-Raman spectrum change compared to the RRS spectrum with the band at 1167 cm^{-1} (C_{10}–C_{11} stretch), gaining intensity relative to the band at 1200 cm^{-1} (C_{14}–C_{15} stretch) (Smith et al., 1987b) in the FT-Raman spectrum.

The FT-Raman and RRS of the mutant Y185F (Figure 1c,d, respectively) are also in good agreement with each other with the exception of the changes noted above. *In contrast, a comparison of the corresponding FT-Raman and RRS of bR and Y185F reveals significant differences.* For example, the 959-cm^{-1} band assigned to the C_{11}–H and C_{12}–H hydrogen-out-of-plane (HOOP) mode of the chromophore is intensified in *both* the FT-Raman and RRS of Y185F relative to the corresponding spectra in bR (957 cm^{-1} in FT-Raman, 958 cm^{-1} in RRS). A similar effect is observed for the 1169-cm^{-1} band of Y185F. Changes are also observed between bR and Y185F in the FT-Raman and RRS spectra for the ethylenic mode (C=C stretch) (1526 cm^{-1} in wild-type bR and near 1528 cm^{-1} in Y185F). In the case of bR, the full width at half-maximum (FWHM) of this band is much narrower (FT-Raman, 16 cm^{-1}; RRS, 17 cm^{-1}) compared to the Y185F ethylenic band (FT-Raman, 26.5 cm^{-1}; RRS, 27 cm^{-1}). This effect, as seen in the expanded region around the ethylenic band (Figure 2), is mainly due to the presence of a subcomponent band at 1518 cm^{-1} in Y185F which is not detected in bR. This additional band is seen more clearly in the deconvoluted spectrum of Y185F (inset to Figure 2).

There are also additional features in the RRS spectrum of Y185F relative to WT which are not observed in the corresponding FT-Raman spectrum. As discussed later, this is due to the effect of the exciting visible laser beam (568.2 nm) which causes photoconversion of an O-like (O^{Y185F}) species present in Y185F. These changes include increased intensities for bands at 1186, 1439, 1529, and 1547 cm^{-1} (Figures 1 and 2) and also a downshifted methyl rocking mode from 1007 cm^{-1} (in FT-Raman) to 1006 cm^{-1}, characteristics of the N intermediate of the bR photocycle (Fodor et al., 1988; Nakagawa et al., 1991).

In the case of the FT-Raman spectrum, where photoreactions are not expected and thus do not contribute to the spectrum, changes observed in the Y185F spectra relative to the bR spectra are most likely due to the presence of stable species in addition to bR_{570}. In order to determine the contribution due to these species, we interactively subtracted

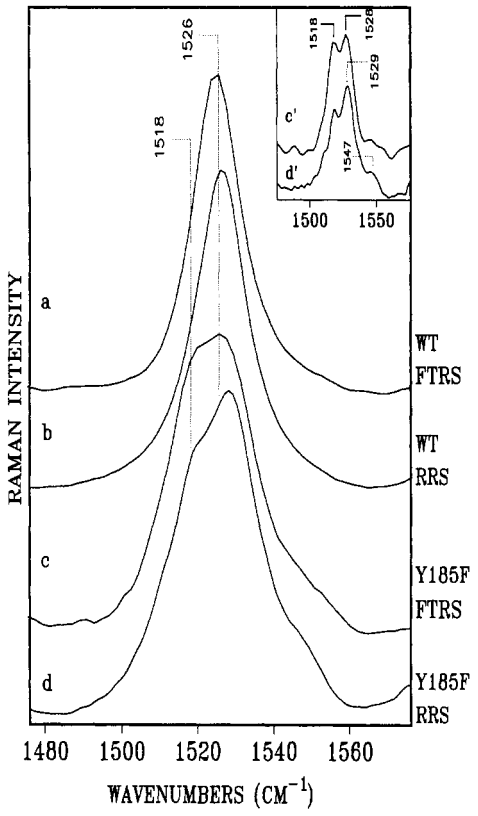

FIGURE 2: Expanded view of the ethylenic region of the FT-Raman and resonance Raman spectra. Spectra shown are the same as in Figure 1 but in the region between 1475 and 1575 cm^{-1}. Shoulders on the low-frequency side of the main ethylenic bands of the Y185F spectra (c and d) are clearly visible. Inset: Spectra c and d are presented (as c′ and d′, respectively) after deconvolution, showing the presence of a band at 1518 cm^{-1}. A commercially available software, LabAalc (Galactic Industries, Nasua, NH), was used for Fourier self-deconvolution of the spectra. The parameters used were γ = 1.5 and filter = 0.5.

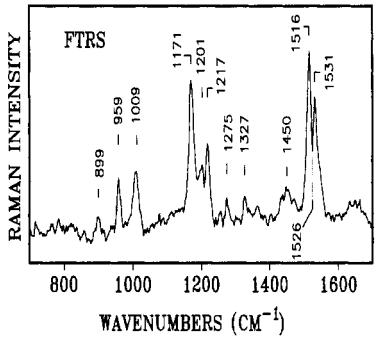

FIGURE 3: Interactive subtraction of the wild-type bR FT-Raman spectrum from that of Y185F. The subtraction factor was chosen to obtain maximum subtraction of the bR_{570} component bands in Y185F without creating negative bands in the fingerprint (1100–1400 cm^{-1}) or HOOP regions. The positive bands that appear are mainly due to the chromophore vibrations of an O-like species (O^{Y185F}) present in the light-adapted Y185F.

the FT-Raman bR spectrum from the corresponding Y185F spectrum. (The subtraction factor was chosen so as to have minimum contribution of bR_{570} in the result without producing any negative bands either in the HOOP or in the fingerprint region.) The result of this subtraction (Figure 3) exhibits positive bands at 1009, 1171, 1201, 1217, 1275, 1327, and 1450 cm^{-1} and in the HOOP mode region at 899 and 959 cm^{-1}, close to the frequency of major bands in the RRS spectrum of the O intermediate (Smith et al., 1983; Ames & Mathies, 1990). Especially noticeable is the strong intensity of the 1171- and 959-cm^{-1} bands characteristic of the O intermediate which has a distorted all-trans structure (Smith et al., 1983; Ames & Mathies, 1990). *Since the frequency of the bands in these regions is very sensitive to chromophore structure, this comparison indicates that the second species present in light-adapted Y185F is similar to the O intermediate, in agreement with a related study using low-temperature FTIR difference spectroscopy (He et al., 1993).* Note that in the ethylenic region (Figure 3), a positive band appears at 1516 cm^{-1} [with a shoulder near 1510 cm^{-1}], 6 cm^{-1} above that observed in the RRS of the O intermediate. In comparison, ethylenic bands are found by FTIR to be split and located at 1510 and 1520 cm^{-1} (He et al., 1993). However, these bands may not be resolved in the FT-Raman spectra because of the lower resolution. In addition, this region is masked in the FT-Raman Y185F – WT subtraction (Figure 3) due to the presence of bands near 1526 (negative) and 1531 cm^{-1}, which arise from an intrinsic shift in the ethylenic mode of the bR_{570}-like species in Y185F relative to wild-type bR. A similar effect is also observed in a Y185F – WT subtraction for the low-temperature FTIR spectra (He et al., 1993). A similar problem does not occur when the same procedure is used for the visible absorption (Sonar et al., 1993) because the absorption bands are much broader relative to the shifts that occur.

FT-Raman Spectra of Dark-Adapted Y185F. The FT-Raman spectrum of dark-adapted bR (Figure 4a) agrees well with a previously reported result (Sawatzki et al., 1990). Bands characteristic of both the *all-trans*-retinal bR (bR_{570}) species (957, 1167, 1200, and 1321 cm^{-1}) and the 13-cis, C=N syn retinal (bR_{555}) species (798, 1180, and 1342 cm^{-1}) appear, reflecting the presence of both of these species in dark-adapted bR (Marcus & Lewis, 1978; Aton et al., 1979; Stockburger et al., 1979; Terner et al., 1979; Smith et al., 1983, 1984, 1987a). An expansion of the ethylenic region (Figure 4a′, inset) also shows subcomponent bands at 1528 and 1533 cm^{-1} due to the bR_{570} and bR_{555} components, respectively.

In contrast to dark-adapted bR, the corresponding dark-adapted Y185F spectrum (Figure 4c) has significantly less contribution from the *all-trans*-bR_{570} species (bR_{570}^{Y185F}). This can be seen from the fingerprint region (1100–1400 cm^{-1}), which is very similar to the RRS spectrum of pure bR_{555} (Terner et al., 1979; Stockburger et al., 1979; Smith et al., 1983, 1984, 1987a) (see below), as well as from the increased intensity of the 797-cm^{-1} band and the drop in intensity of the ethylenic band at 1528 cm^{-1} (see inset, Figure 4c′).

It is possible to obtain the pure 13-cis component of the dark-adapted bR and Y185F spectra by interactively subtracting the corresponding light-adapted spectra. Both resulting subtractions (Figure 4b,d) are very similar to the resonance Raman spectrum of the 13-*cis*-bR_{555} (Terner et al., 1979; Stockburger et al., 1979; Smith et al., 1983, 1984, 1987a), verifying that this species is present in both dark-adapted bR and Y185F. However, a shift is found in the frequency of the main ethylenic band of Y185F relative to wild-type bR from 1534 to 1538 cm^{-1} (Figure 4d), in agreement with the blue shift observed in the λ_{max} of the dark-adapted samples from 555 to 548 nm (Sonar et al., 1993).

Notice that in contrast to dark-adapted wild-type bR (Figure 4a′), a shoulder appears near 1518 cm^{-1} in Y185F (inset, Figure 4c′) which indicates the presence of a red-shifted species. Such a red-shifted species is in fact detected by visible absorption spectroscopy (Sonar et al., 1993) and has been attributed to an equilibrium between a bR_{570} and an O-like species in the all-trans component of dark-adapted Y185F. A

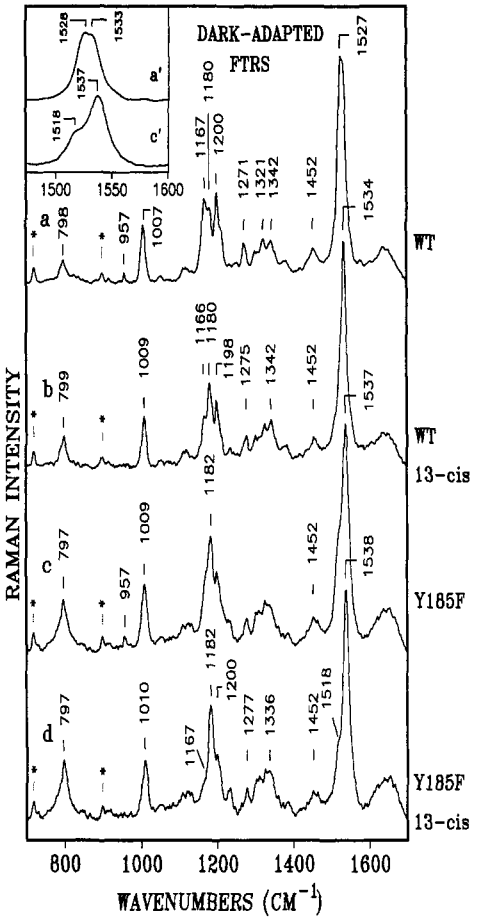

FIGURE 4: FT-Raman spectra of dark-adapted wild-type bR and Y185F. Dark-adapted spectra shown are (a) for wild-type bR and (c) for Y185 at 4-cm^{-1} resolution. The spectrum for the dark-adapted wild-type bR resembles the RRS of bR_{555} (Smith et al., 1987a). The inset shows shoulders at 1533 cm^{-1} for wild-type bR (a') and at 1537 cm^{-1} for the mutant Y185F (c') due to the ethylenic bands from the 13-cis component of the dark-adapted sample. Spectra b and d were computed by interactively subtracting out the contribution from the fully light-adapted samples (Figure 1a,c) to give pure spectra of the 13-cis species present in the dark-adapted sample. Bands marked with an asterisk are due to spectrometer artifacts.

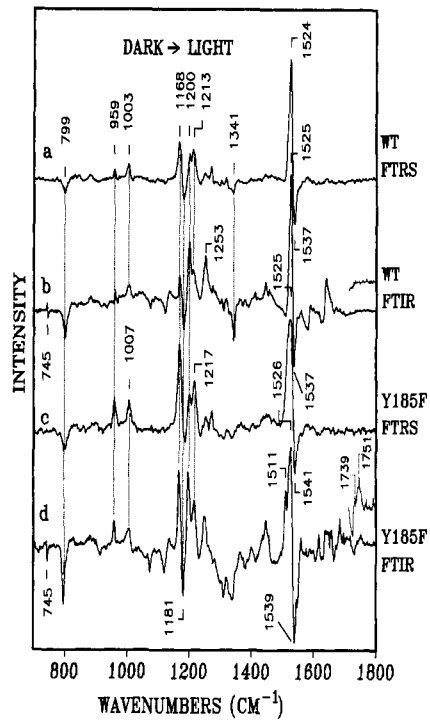

FIGURE 5: Dark→light difference spectra. Fourier transform Raman spectroscopy (FTRS) and FTIR difference spectra for the light adaptation of wild-type bR samples (a and b, respectively) and Y185F (c and d, respectively) are shown. FTRS spectra were recorded at 4-cm^{-1} resolution at room temperature, whereas the FTIR spectra were recorded at 2-cm^{-1} resolution and at 310 K for wild-type bR (Roepe et al., 1988) and at 293 K for Y185F. A 3 times expanded y scale in the 1720–1800-cm^{-1} region is shown for FTIR difference spectra.

fraction of this band, however, may also be due to an intrinsic vibrational band in bR_{555} which has been assigned to a combination of C_{13}=C_{14} and C_9=C_{10} stretching modes (Smith et al., 1987a). This band would account for the presence of a 1518-cm^{-1} component at a reduced intensity in the pure bR_{555} spectrum of dark-adapted Y185F (Figure 4d).

Light and Dark Adaptation of Y185F. FT-Raman spectroscopy was used to measure the light adaptation reaction of wild-type bR and the mutant Y185F. In wild-type bR, the largest change expected is a shift in the frequency of the ethylenic band from 1534 to 1527 cm^{-1}, reflecting the conversion of bR_{555} to bR_{570}. As seen in Figure 5a, this results in a FT-Raman dark→light difference spectrum with a pair of bands at 1537 cm^{-1} (negative) and 1524 cm^{-1} (positive). Note that due to the overlap, these bands appear in the difference spectrum with higher (1537 cm^{-1}) and lower (1524 cm^{-1}) frequencies than the actual frequencies of the ethylenic bands in bR_{555} and bR_{570}, respectively. A second prominent feature of the dark→light difference spectrum is the negative band near 799 cm^{-1} which is due to the $C_{14}H$ HOOP mode in bR_{555} (Smith et al., 1987a). We also show for comparison the dark→light difference spectrum obtained from FTIR difference spectroscopy of wild-type bR (Figure 5b) in a hydrated film at 310 K (Roepe et al., 1988). The agreement in the frequency of bands assigned to the chromophore is very good, whereas differences occur mainly at the frequency of bands assigned to protein vibrations such as at 1253 cm^{-1} (amide III) and 745 cm^{-1} (Trp-86) (Rothschild et al., 1989).

The dark→light FT-Raman difference spectrum of the mutant Y185F is shown in Figure 5c. This spectrum is similar to that of bR, especially in the C–C stretching fingerprint region (1100–1400 cm^{-1}), demonstrating that the Y185F chromophore undergoes the same structural change, a 13-cis, C=N syn to all-trans isomerization during light adaptation (Marcus & Lewis, 1978; Smith et al., 1984; Lugtenburg et al., 1988). However, the relative intensities of bands at 959 and 1168 cm^{-1} in this spectrum compared to wild-type bR (Figure 5a) are significantly increased. In addition, the positive ethylenic band at 1525 cm^{-1} is much broader. Expansion of this region (not shown) reveals that it contains a shoulder near 1520 cm^{-1}. As pointed out earlier, all of these bands are associated with the presence of an O-like species in the light-adapted Y185F. *Their appearance in the dark→light difference spectrum indicates that along with* bR_{570}^{Y185F}, O^{Y185F} *also forms during light adaptation.* A similar pattern is also observed in the dark→light FTIR difference spectrum for Y185F (Figure 5d) compared to wild-type bR (Figure 5b), with new spectral features observed at the same positions as in the FT-Raman difference spectrum of Y185F. Note that a band at 1511 cm^{-1} characteristic of the O intermediate is also observed in Figure 5d, possibly due to the higher resolution of the FTIR measurements (2 cm^{-1}) compared to the FT-Raman measurements (4 cm^{-1}).

The appearance of the band at 1751 cm^{-1} with a small shoulder at 1739 cm^{-1} in the dark→light FTIR difference spectrum of Y185F (Figure 5d) and their absence in the wild-

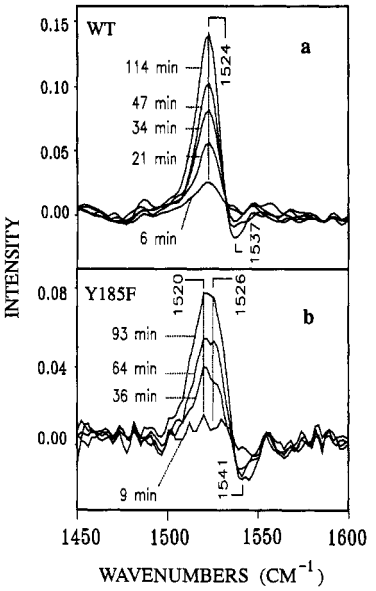

FIGURE 6: Time-resolved FT-Raman light→dark difference spectra. Difference spectra were computed by subtracting the spectrum of the sample recorded at various times in the dark after light adaptation from that of the spectrum of a light-adapted sample. Difference spectra shown are at 8-cm^{-1} resolution.

type bR difference spectrum are especially interesting since these bands have been assigned previously to the carboxyl (COOH) stretch mode of Asp-85 and Asp-212, respectively, in the O intermediate (Bousché et al., 1992). *This confirms that the O^{Y185F} species formed upon light adaptation of Y185F has an identical protonation state of these Asp residues as that of the O intermediate.* In contrast, the dark→light FTIR differnece spectrum of wild-type bR (Figure 5b) does not exhibit such bands, consistent with the model that the protonation state of these residues does not change during light adaptation (see Discussion).

In order to determine the relative rate of dark adaptation in bR and Y185F, the sample was light-adapted, and then difference spectra were recorded between the light-adapted sample and the same at subsequent times during the thermal dark adaptation reaction. As seen in the difference spectra in Figure 6a, the 1524-cm^{-1} peak increases in intensity as the bR_{570} species decays, accompanied by an increase in the negative 1537-cm^{-1} band corresponding to the formation of the bR_{555} species. The increase at 1524 cm^{-1} was fit by a single-exponential curve with a $t_{1/2}$ of 28 min. Similar difference spectra were obtained for the Y185F sample and are shown in Figure 6b. In contrast to wild-type bR, Y185F exhibits a much slower dark adaptation rate, which is reflected by the growth of *two bands* at approximately 1519 and 1526 cm^{-1}. Due to insufficient time points, we were not able to determine an accurate decay rate or to see if the decay was single-exponential. However, experiments using visible absorption spectroscopy confirmed that there exists a parallel decay of the two species. In this case, a decay rate at room temperature was found to be 12 h (Sonar et al., 1993). Similar results were also obtained using FTIR difference spectroscopy (Y. W. He and K. J. Rothschild, unpublished data).

Detection of a Transient N Photoproduct of the O^{Y185F} Photoreaction. We investigated the photoproduct of the O^{Y185F} species using a pump–probe technique, where the RRS of a spinning sample of Y185F at pH 6.8 was measured with and without exposure to a red 647.1-nm pump laser beam (see Materials and Methods). Since the O^{Y185F} species absorbs near the wavelength of the pump beam, the RRS difference

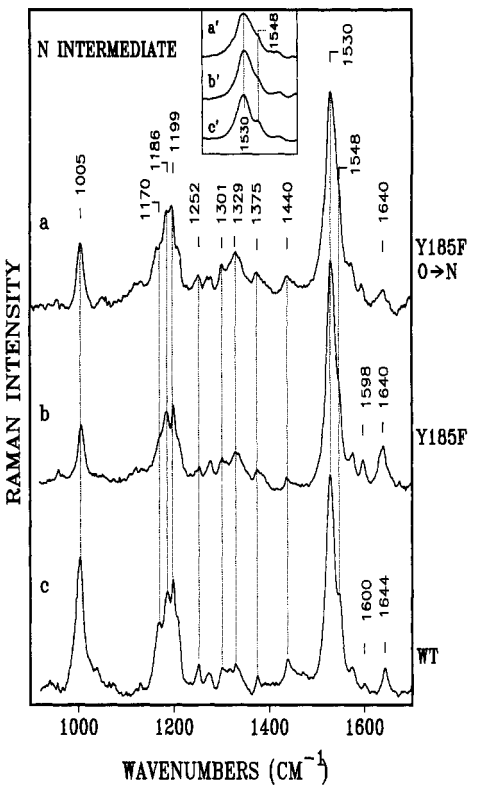

FIGURE 7: Resonance Raman spectra of the N intermediate. Spectrum a was obtained by photoconverting the O^{Y185F} species of Y185F at pH 6.8 with a 100-mW 647.1-nm pump beam at 5 ms upstream and measured using a 5-mW 514.5-nm probe beam; (b) spinning sample of Y185F at pH 9 (30 mM sodium phosphate buffer), probed with a 5-mW 514.5-nm probe beam; (c) wild-type sample in a spinning cell at pH 9 (10 mM Tris) and 3 M KCl, probed with a 2-mW 520.8-nm probe beam (see Materials and Methods).

spectrum obtained should reflect the photoproduct of this species. As seen in Figure 7a (difference between pump+probe and probe-only spectrum), a prominent band at 1186 cm^{-1} characteristic of a 13-cis-containing species is observed in this difference spectrum. In contrast, a control experiment on wild-type bR did not show any change in the Raman spectrum in the presence of the pump beam (data not shown). Significantly, the Y185F pump–probe difference spectrum is very similar to the RRS spectrum of the N intermediate from the photocycle of Y185F (Figure 7b) and also the N intermediate of wild-type bR (Figure 7c) obtained by subtraction of the pH 7 wild-type bR spectrum from that of pH 9 (see Materials and Methods). In addition to the 1186-cm^{-1} band, all of the spectra shown in Figure 7 exhibit bands previously reported as characteristic of the Raman spectrum of the N intermediate (Fodor et al., 1988; Nakagawa et al., 1991), including a characteristic split ethylenic at 1530 and 1548 cm^{-1} (see inset) and additional bands near 1005, 1170, 1199, 1329, and 1440 cm^{-1}. Note that the 1644-cm^{-1} band in the N intermediate of wild-type bR (Figure 7c), assigned to the C=N stretch mode of the protonated Schiff base (Fodor et al., 1988), is downshifted by 4 cm^{-1} in the corresponding spectrum for the N intermediate of Y185F. A similar downshift also appears to occur in the C=N stretch mode of the bR_{570} species of Y185F compared to wild-type bR in the resonance Raman spectra (Figure 8a, see below) and FTIR difference spectra (He et al., 1993). Although the RRS of the L intermediate is similar to the N intermediate (Maeda et al., 1986; Nakagawa et al., 1991), it is unlikely that this species contributes to the difference spectrum shown in Figure 7a since the time constant for L decay in Y185F (16

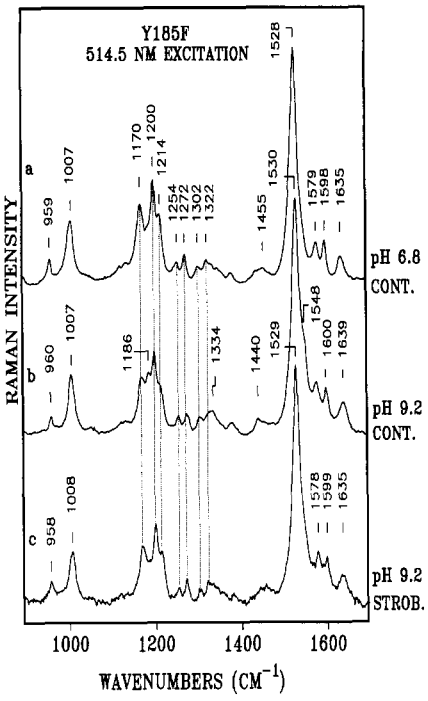

FIGURE 8: Resonance Raman spectra of Y185F at neutral and high pH. Spectra from a spinning sample of Y185F at pH 6.8 (a) and pH 9.2 (b and c) were obtained with continuous illumination by a 5-mW, 514.5-nm probe beam (a and b), whereas (c) was recorded with a stroboscopic 514.5-nm probe beam which was switched on for 0.1 s and then switched off for 1.9 s during which time data are not recorded (see Materials and Methods).

μs) (Sonar et al., 1993) is much shorter than the time for the sample to complete one rotation in the spinning cell (22 ms). Because the pump beam, which excites the O^{Y185F} species, is focused upstream of the probe beam, only photointermediates which have a lifetime as long as 5 ms will contribute significantly to the difference spectrum (see Materials and Methods).

As a control, spectra recorded using a low-power probe beam at 514.5 nm, which is not absorbed strongly by the O^{Y185F} species, resulted in RRS which showed little or no contribution from the N intermediate. For example, the RRS of Y185F recorded at pH 6.8 using 5-mW power (Figure 8a) shows no detectable contributions from bands associated with the N intermediate. In contrast, a similar spectrum recorded using 568.2-nm excitation (Figure 1d) resulted in contributions from both O^{Y185F} and the N intermediate (see above). In this case, O^{Y185F} is observed because there is increased resonance enhancement of this species relative to the RRS of Y185F recorded with 514.5-nm excitation, and N is formed because of photoexcitation of O^{Y185F} by the 568.2-nm probe beam.

A similar measurement as described above using low-power 514.5-nm excitation was made for Y185F at pH 9.2, where decay of the N intermediate is expected to be much slower than at pH 6.8 (Kouyama et al., 1988). As seen in Figure 8b, bands now appear near 1186 and 1548 cm^{-1}, confirming the presence of the N intermediate in the sample under these conditions. However, if the RRS spectrum is measured under the same conditions using a stroboscopic probe beam (0.1-s on followed by 1.9-s off), no N intermediate bands are detected (Figure 8c). In this case, the spectrum is almost identical to that measured at pH 6.8 (Figure 8a). Hence, under these conditions, any N intermediate which accumulates due to sample excitation must decay in under 1.9 s or else it would appear in the stroboscopic spectrum. *Thus, we can conclude that even at pH 9.2, there is no significant N intermediate present in light-adapted Y185F except for transient N accumulation during the photocycle.*

DISCUSSION

In this work, we have used FT-Raman spectroscopy to study the light–dark adaptation of bR and its mutant Y185F. Since the near-infrared 1064-nm beam from a CW Nd-YAG laser produces Raman scattering, far from the main absorption of the bR chromophore and its photointermediates, the problem of sample photoexcitation which normally occurs with conventional resonance Raman spectroscopy is eliminated. For example, in order to measure the resonance Raman spectrum of dark-adapted bR, it is necessary to use a flowing sample which avoids contributions due to light adaptation from the probe beam (Marcus & Lewis, 1978; Aton et al., 1979; Terner et al., 1979; Stockburger et al., 1979; Smith et al., 1983, 1984, 1987a). In the case of FT-Raman, however, it is possible to measure the Raman spectrum of both light- and dark-adapted Y185F using a static sample. The signal-to-noise ratio obtainable with the Bio-Rad FTS 40 spectrometer equipped with a liquid nitrogen cooled Ge detector was sufficient to acquire individual difference spectra during dark adaptation with 2-min time resolution and 4-cm^{-1} spectral resolution.

Our results confirm that a stable red-shifted species exists in light-adapted Y185F which has a vibrational spectrum similar to the O intermediate of the wild-type bR photocycle. Since Y185F was produced in purple membrane patches isolated from the native *H. halobium* (see Materials and Methods), the presence of O^{Y185F} is not likely to be a product of a nonnative membrane environment. Furthermore, the O^{Y185F} species was measured at room temperature at pH 7, well above the pK_a of 3.7 for the acid-induced blue transition of Y185F (Sonar et al., 1993). *We therefore conclude that the existence of the O^{Y185F} species in light-adapted Y185F is an intrinsic property of this mutant and is likely to reflect an equilibrium which exists between bR_{570}^{Y185F} and the O^{Y185F} intermediate, in agreement with the conclusions based on visible absorption spectroscopy (Sonar et al., 1993).* Our studies also reveal several other properties of the light- and dark-adapted states of Y185F which are summarized below:

The O^{Y185F} Species Is Formed during Light Adaptation. In related studies using visible absorption spectroscopy (Duñach et al., 1990; Sonar et al., 1993), it was demonstrated that a red-shifted intermediate is formed along with the normal bR_{570}-like species during light adaptation of Y185F. However, visible absorption spectra do not provide information about the chromophore structure of this species. In the present study, we found that both the dark→light FT-Raman and FTIR difference spectra of Y185F are very similar to wild-type bR, reflecting a 13–cis, C=N syn→all-trans isomerization of the chromophore. However, additional bands were also detected in the dark→light difference spectrum which reflect formation of an O-like species. This confirms that light adaptation in Y185F produces, from a bR_{555}-like species, two all-trans species similar to bR_{570} and the O intermediate.

Dark-Adapted Y185F Has an Increased Content of 13-cis-Retinal Isomer. FT-Raman spectra demonstrate that there is a significant increase in the 13-cis, C=N syn isomer content relative to wild-type bR. In addition, we found that a frequency shift occurs in the C=C stretch mode of the 13-cis component (from 1534 to 1538 cm^{-1}), consistent with a blue shift in its λ_{max} from 555 to 548 nm as observed using visible absorption spectroscopy (Sonar et al., 1993). Thus, Tyr-185 appears to play a critical role in the relative stability of the two forms of the chromophore in the dark-adapted system as well as in its interaction with the chromophore in the 13-cis form.

Dark Adaptation Is Very Slow in Y185F Relative to WT. In agreement with the results from visible absorption spectroscopy (Duñach et al., 1990; Sonar et al., 1993), we observe a dark adaptation rate for Y185F which is much slower than wild-type bR. This result points to the importance of the residue Tyr-185 in dark adaptation. As previously discussed, this may be due to the disruption of the Tyr-185/Asp-212 hydrogen bond in Y185F (Rothschild et al., 1990; Duñach et al., 1990).

O^{Y185F} and bR_{570}^{Y185F} Decay in Parallel during Dark Adaptation. The FT-Raman difference spectra for dark adaptation of Y185F revealed that both of the all-trans species, bR_{570}^{Y185F} and O^{Y185F}, decay with similar time constants, consistent with the results from visible absorption spectroscopy (Sonar et al., 1993) and FTIR difference spectroscopy (unpublished results). One explanation for these results is the existence of an equilibrium between bR_{570}^{Y185F} and the O^{Y185F} species. In this case, decay of bR_{570}^{Y185F} to bR_{555}^{Y185F} is expected to cause a net conversion of the O^{Y185F} species to bR_{570}^{Y185F} so that the O^{Y185F}:bR_{570}^{Y185F} ratio remains constant during dark adaptation.

The O^{Y185F} Species Has a Transient N Photoproduct at Room Temperature. Strong evidence for the existence of the O^{Y185F} species in light-adapted Y185F comes from the finding that photoexcitation by red light causes an accumulation of a transient species with a chromophore structure very similar to the N intermediate whereas an N-like species is not detected under conditions where O^{Y185F} is not photoexcited. This explains why we observe accumulation of a transient N-like species in the resonance Raman spectrum of Y185F using 568-nm excitation. The result also places a limit on the amount of the N species which could be in equilibrium with the O^{Y185F} species. We are also able to exclude the possibility (Sonar et al., 1993) that at high pH the O^{Y185F} species is converted into a stable N-like intermediate since this species was not detected even at high pH by stroboscopic resonance Raman spectroscopy. Our results also indicate that the O^{Y185F} photocycle involves a long-lived N intermediate ($t_{1/2}$ comparable to 5 ms at pH 6.8) which cycles back to O^{Y185F} either directly or through a branch involving bR_{570}^{Y185F} (Sonar et al., 1993; He et al., 1993).

The Protonation States of Key Asp Residues of the O^{Y185F} Species Formed during Light Adaptation and That of the O Intermediate Are Similar. Dark→light FTIR difference spectra demonstrate that the residues Asp-85 and Asp-212 are protonated in the O^{Y185F} species of light-adapted Y185F. A similar conclusion was also reached for the transient O photoproduct of Y185F on the basis of room temperature FTIR difference spectroscopy (Bousché et al., 1992). This evidence provides further support for similar structures of the O^{Y185F} species and the O intermediate of the Y185F photocycle. The protonation of Asp-212 in Y185F could be explained by the presence of a water molecule which substitutes for the hydroxyl group of Tyr-185 as previously postulated (Rothschild et al., 1990; Bousché et al., 1992).

Molecular Model for the Equilibrium between Different Stable bR States. Dark-adapted bR consists of two species corresponding to 13-cis and all-trans isomers of the chromophore in an approximately 65:35 ratio (Scherrer et al., 1989). A similar mixture of 13-cis and all-trans isomers exists for acid-induced blue membrane (Mowery et al., 1979; Fischer & Oesterhelt, 1979). In the acid-induced transition, both species convert to form blue membrane, which has been observed to occur with a pK_a near 2.6 but is a function of ionic concentration (Oesterhelt & Stoeckenius, 1971; Ohno et al., 1977; Mowery et al., 1979; Muccio & Cassim, 1979; Ohtani et al., 1986; Smith & Mathies, 1985; Massig et al., 1985). Evidence also indicates that Asp–85 undergoes a protonation during this transition (Subramaniam et al., 1990; Marrero & Rothschild, 1987, Rothschild, 1992), thus accounting for its red-shifted absorption maximum. However, attempts to study the acid-induced transition for pure species of all-trans and 13-cis isomers of bR are more difficult. For example, in the case of the *all-trans*-bR_{570} species, the high rate of dark adaptation at low pH (Ohno et al., 1977; Mowery et al., 1979; Mathew et al., 1986) prevents the pure transition from being observed. In addition, no data exist on the acid-induced transition for the pure 13-cis species. Recently, however, information about the photoreactions of the all-trans species of acid-induced blue membrane (BM^T) has been obtained using FTIR difference spectroscopy (Fahmy & Siebert, 1990).

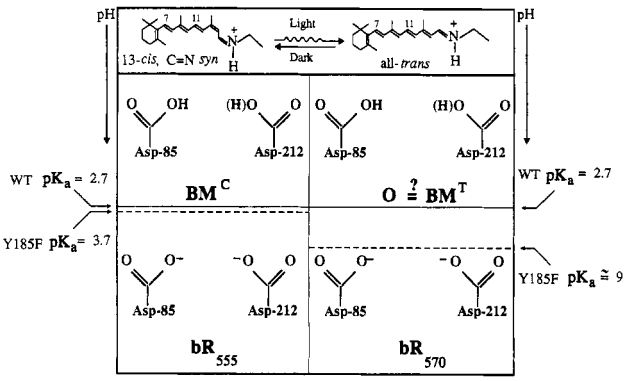

FIGURE 9: Ionization states of Asp-85 and Asp-212 residues in wild-type bR and Y185F. Model showing the ionization states of the Asp residues for different stable bR species as a function of pH and light. Transition between the various stable states of bR occurs by light adaptation (left→right) or increasing pH (top→bottom). The acid-induced blue transition due to lowering of the pH occurs at the solid line boundary (—) for wild type and at the dashed line boundary (– –) for Y185F. (H) denotes partial protonation. The possible equivalence of BM^T and the O species is indicated. The pK_a values shown are as reported in the preceding paper (Sonar et al., 1993).

In the context of the above discussion, we illustrate in Figure 9 the possible structure and dependence on pH and light of the various bR states observed for wild-type bR and Y185F. Importantly, we have treated the transition of the all-trans and 13-cis species separately, resulting in four separate species as a function of light and pH. In the right column are shown the bR_{570} and O species, both of which contain all-trans chromophore. As discussed, the bR_{570} to O transition involves the protonation of Asp-85 and partial protonation of Asp-212 (Bousché et al., 1992). Furthermore, since the FTIR difference spectra for the BM^T to L transition at low temperature (Fahmy & Siebert, 1990) and the O→N transition in Y185F at room temperature (Bousché et al., 1992) are similar, we indicate that the O-like species may be equivalent to the all-trans component of acid-induced blue membrane, BM^T, although further measurements will be necessary to check this possibility.

On the left side of the diagram are listed the two 13-cis chromophore-containing species which exist in the dark. The bR_{555} species, shown on the bottom left, is found in wild-type bR at a pH above 2.7 (Sonar et al., 1993). Like in bR_{570}, the two key Asp residues near the active site, Asp-85 and Asp-212, are ionized in this species, since bands associated with protonation changes of these groups are not observed in the light-dark FTIR difference spectrum (Figure 5b) (Roepe et al., 1988). Below pH 2.7, we postulate that the 13-cis-containing isomer of acid-induced blue membrane (BM^C) is

formed directly from bR_{555}. Because of the similar red shift which occurs for this transition and the bR_{570} to BM^T transition (approximately 60 nm), it is possible that both transitions involve a similar protonation reaction of the residues Asp-85 and Asp-212.

Although the pK_a's of the acid-induced blue transition for the all-trans and 13-cis components of bR have not been determined individually, in the context of the scheme presented in Figure 9, most of the properties of Y185F can be explained simply as due to a relatively large increase in the pK_a for the acid-induced transition of the all-trans component of Y185F and only a small increase for the 13-cis component. For example, such an increase would explain why an O-like species (BM^T) is observed at neutral pH. In contrast, a significant amount of BM^C is not observed in dark-adapted Y185F, consistent with the acid-induced blue transition for the 13-cis forms remaining largely unchanged. As discussed, the residual red-shifted species observed in the dark may be due to the all-*trans*-bR_{570} component which is in equilibrium with the O intermediate (BM^T). Further studies, however, will be necessary to confirm this.

On a molecular level, the increase in the pK_a for the acid-induced bR_{570} to O (BM^T) transition may be related to the disruption of the hydrogen bond between Tyr-185 and Asp-212. The removal of this bond should act to destabilize the ionized state of Asp-212 and act to raise its effective pK_a relative to wild-type bR. However, conformational coupling between various groups in the active site of bR may not allow Asp-212 to undergo a protonation change without a parallel protonation change of Asp-85. For example, the linkage between the two Asp groups (85 and 212) might involve movement of the protonated Schiff base and associated Lys-216 side chain, along with twisting around the C–C bonds of the chromophore. Indeed, the RRS of the O intermediate shows intensified HOOP modes characteristic of conformational strain in the polyene chain (Smith et al., 1983). Further studies will be necessary in order to establish if such coupling does exist.

CONCLUSIONS

We have demonstrated in this work the usefulness of FT-Raman spectroscopy for studying bacteriorhodopsin and its mutants. The ability to study light–dark adaptation as well as other photoreaction without using visible light as a probe provides a powerful complement to other vibrational methods such as FTIR and resonance Raman spectroscopy. As shown in the present work, we are able to detect the presence of a stable O-like species which exists along with bR_{570} in light-adapted Y185F. Similar studies using FT-Raman spectroscopy can now answer the question of whether other bR mutants also exhibit this property. As discussed here [and also in Sonar et al. (1993) and He et al. (1993)], this may reflect a molecular defect which allows the O intermediate to exist in equilibrium with bR_{570}.

ACKNOWLEDGMENT

We thank Drs. D. Compton, D. Drapcho, and B. Smith of Bio-Rad, Digilab Division, for valuable technical help and providing the use of an FTS-40 FT-Raman spectrometer. We also thank Drs. S. Sonar and W. Fischer for many valuable suggestions.

REFERENCES

Ames, J. B., & Mathies, R. A. (1990) *Biochemistry 29*, 7181–7190.

Argade, P. V., & Rothschild, K. J. (1982) *Methods Enzymol. 88*, 643–648.

Aton, B., Doukas, A., Callender, R., Becher, B., & Ebrey, T. (1979) *Biochim. Biophys. Acta 576*, 424–428.

Bagley, K., Dollinger, G., Eisenstein, L., Singh, A. K., & Zimanyi, L. (1982) *Proc. Natl. Acad. Sci. U.S.A. 79*, 4972–4976.

Bousché, O., Sonar, S., Krebs, M., Khorana, H. G., & Rothschild, K. J. (1992) *Photochem. Photobiol. 56*, 1085–1095.

Braiman, M. S., Mogi, T., Marti, T., Stern, L. J., Khorana, H. G., & Rothschild, K. J. (1988a) *Biochemistry 27*, 8516–8520.

Braiman, M. S., Mogi, T., Stern, L. J., Hackett, N. R., Chao, B. H., Khorana, H. G., & Rothschild, K. J. (1988b) *Proteins: Struct., Funct., Genet. 3*, 219–229.

Callender, R., & Honig, B. (1977) *Annu. Rev. Biophys. Bioeng. 6*, 33–55.

Callender, R., Doukas, A., Crouch, R., & Nakanishi, K. (1976) *Biochemistry 15*, 1621–1629.

Deng, H., Pande, C., Callender, R., & Ebrey, T. (1985) *Photochem. Photobiol. 41*, 467–470.

Duñach, M., Berkowitz, S., Marti, T., He, Y. W., Subramaniam, S., Khorana, H. G., & Rothschild, K. J. (1990) *J. Biol. Chem. 265*, 16978–16984.

Engelhard, M., Gerwert, K., Hess, B., Kreutz, W., & Siebert, F. (1985) *Biochemistry 24*, 400–407.

Fahmy, K., & Siebert, F. (1990) *Photochem. Photobiol. 51*, 459–464.

Fischer, U., & Oesterhelt, D. (1979) *Biophys. J. 28*, 211–230.

Fodor, S., Ames, J., Gebhard, R., van den Berg, E., Stoeckenius, W., Lugtenburg, J., & Mathies, R. (1988) *Biochemistry 27*, 7097–7101.

Gerwert, K., Hess, B., Soppa, J., & Oesterhelt, D. (1989) *Proc. Natl. Acad. Sci. U.S.A. 86*, 4943–4947.

He, Y., Krebs, M. P., Fischer, W. B., Khorana, H. G., & Rothschild, K. J. (1993) *Biochemistry* (third of three papers in this issue).

Johnson, C. K., & Rubinovitz, R. (1990) *Appl. Spectrosc. 44*, 1103–1106.

Kouyama, T., Nasuda-Kouyama, A., Ikegami, A., Mathew, M., & Stoeckenius, W. (1988) *Biochemistry 27*, 5855–5863.

Lugtenburg, J., Mathies, R. A., Griffin, R. G., & Herzfeld, J. (1988) *Trends. Biochem. Sci. (Pers Ed.) 13*, 388–393.

Maeda, A. T., Ogura, T., & Kitagawa, T. (1986) *Biochemistry 25*, 2798–2803.

Maeda, A., Sasaki, J., Shichida, Y., Yoshizawa, T., Chang, M., Ni, B., Needleman, R., & Lanyi, J. K. (1992) *Biochemistry 31*, 4684–4690.

Marcus, M. A., & Lewis, A. (1978) *Biochemistry 17*, 4722–4735.

Marrero, H., & Rothschild, K. J. (1987) *FEBS Lett. 223*, 289–293.

Massig, G., Stockburger, M., & Alshuth, T. H. (1985) *Can. J. Chem. 63*, 2012–2017.

Mathew, M., Scherrer, P., Sperling, W., & Stoeckenius, W. (1986) *Biophys. J. 49*, 211a.

Mathies, R. (1979) in *Chemical and Biological Applications of Lasers* (Moore, C. B., Ed.) Vol. IV, pp 55–99, Academic Press, New York.

Mathies, R., Oseroff, A., & Stryer, L. (1976) *Proc. Natl. Acad. Sci. U.S.A. 73*, 1–5.

Mathies, R., Lin, S., Ames, J., & Pollard, W. (1991) *Annu. Rev. Biophys. Biophys. Chem. 20*, 491–518.

Mowery, P. C., Lozier, R. H., Chae, Q., Tseng, Y., Taylor, M., & Stoeckenius, W. (1979) *Biochemistry 18*, 4100–4107.

Muccio, D. D., & Cassim, J. Y. (1979) *J. Mol. Biol. 135*, 595–609.

Myers, A., Harris, R. A., & Mathies, R. (1983) *J. Chem. Phys. 79(2)*, 603–613.

Nakagawa, M., Maeda, A., Ogura, T., & Kitagawa, T. (1991) *J. Mol. Struct. 242*, 221–234.

Oesterhelt, D., & Stoeckenius, W. (1971) *Nature (London), New Biol. 233*, 149–152.

Ohno, K., Takeuchi, Y., & Yoshida, M. (1977) *Biochim. Biophys. Acta 462*, 575–582.

Ohtani, H., Kobayashi, T., Iwai, J., & Ikegami, A. (1986) *Biochemistry 25*, 3356–3363.

Roepe, P. D., Ahl, P. L., Herzfeld, J., Lugtenburg, J., & Rothschild, K. J. (1988) *J. Biol. Chem. 263*, 5110–5117.

Rothschild, K. J. (1992) *J. Bioenerg. Biomembr. 24*, 147–167.

Rothschild, K. J., Zagaeski, M., & Cantore, B. (1981) *Biochem. Biophys. Res. Commun. 103*, 483–489.

Rothschild, K. J., Gray, D., Mogi, T., Marti, T., Braiman, M. S., Stern, L. J., & Khorana, H. G. (1989) *Biochemistry 28*, 7052–7059.

Rothschild, K. J., Braiman, M. S., He, Y. W., Marti, T., & Khorana, H. G. (1990) *J. Biol. Chem. 265*, 16985–16991.

Sawatzki, G., Fischer, R., Scheer, H., & Siebert, F. (1990) *Proc. Natl. Acad. Sci. U.S.A. 87*, 5903–5906.

Scherrer, P., Mathew, M. K., Sperling, W., & Stoeckenius, W. (1989) *Biochemistry 28*, 829–834.

Siebert, F., & Mäntele, W. (1983) *Eur. J. Biochem. 130*, 565–573.

Smith, S. O., & Mathies, R. A. (1985) *Biophys. J. 47*, 251–254.

Smith, S. O., Pardoen, J. A., Mulder, P. P. J., Curry, B., Lugtenburg, J., & Mathies, R. A. (1983) *Biochemistry 22*, 6141–6148.

Smith, S. O., Myers, A. B., Pardoen, J. A., Winkel, C., Mulder, P. P., Lugtenburg, J., & Mathies, R. (1984) *Proc. Natl. Acad. Sci. U.S.A. 81*, 2055–2059.

Smith, S. O., Lugtenburg, J., & Mathies, R. A. (1985) *J. Membr. Biol. 85*, 95–109.

Smith, S., Pardoen, J., Lugtenburg, J., & Mathies, R. (1987a) *J. Phys. Chem. 91*, 804–819.

Smith, S. O., Braiman, M. S., Myers, A. B., Pardoen, J. A., Courtin, J., Winkel, C., Lugtenburg, J., & Mathies, R. A. (1987b) *J. Am. Chem. Soc. 109*, 3108–3125.

Sonar, S., Krebs, M. P., Khorana, H. G., & Rothschild, K. J. (1993) *Biochemistry* (first of three papers in this issue).

Stockburger, M., Klusmann, W., Gattermann, H., Massig, G., & Peters, R. (1979) *Biochemistry 18*, 4886–4900.

Stoeckenius, W., & Bogomolni, R. A. (1982) *Annu. Rev. Biochem. 51*, 587–616.

Subramaniam, S., Marti, T., & Khorana, H. G. (1990) *Proc. Natl. Acad. Sci. U.S.A. 87*, 1013–1017.

Terner, J., Hsieh, C., & El-Sayed, M. (1979) *Biophys. J. 26*, 527–541.

Warshel, A. (1977) *Annu. Rev. Biophys. Bioeng. 6*, 273–300.